Myosin-V colocalizes with MHC class II in blood mononuclear cells and is up-regulated by T-lymphocyte activation

João C. S. Bizario,[*,†] Fabíola A. Castro,[§,‖] Josane F. Sousa,[*] Rafael N. Fernandes,[†] Alexandre D. Damião,[*] Márika K. Oliveira,[*] Patrícia V. B. Palma,[‖] Roy E. Larson,[*] Júlio C. Voltarelli,[‡,‖] and Enilza M. Espreafico[*]

**Departments of Cellular and Molecular Biology and Pathogenic Bioagents, and [‡]Clinical Medicine of the Faculty of Medicine of Ribeirão Preto, and [§]Faculty of Pharmaceutical Sciences of Ribeirão Preto of the University of São Paulo; [†]Medical School of the Ribeirão Preto University (UNAERP), Brazil; and [‖]Blood Center Foundation of Ribeirão Preto, SP, Brazil*

Abstract: Myosin-V is involved in organelle and vesicle trafficking in *Saccharomyces cerevisiae* and in other eukaryotic cells from yeast to human. In the present study, we determined by FACS that the major subpopulations of the peripheral blood mononuclear cells express myosin-V with similar fluorescence intensity. Confocal microscopy showed intense labeling for myosin-V at the centrosomal region and a punctate staining throughout the cytoplasm, frequently associated with the central microtubule arrays and the actin-rich cortex. Some degree of overlap with an endolysosomal marker and dynein light-chain 8 k was found at the cell center. Striking colocalization was observed with the major histocompatibility complex (MHC) class II molecules near the cell surface. Treatment with phytohemagglutinin, which induces T-lymphocyte activation, associated with MHC class II expression, increased the levels of myosin-V protein and mRNA for the three members of class V myosins. These data suggest that class V myosins might be involved in relevant functions in the immune response. *J. Leukoc. Biol.* 71: 195–204; 2002.

Key Words: *Griscelli syndrome · centrosome · natural killer cells · Rab27a · dilute gene · endosomes*

INTRODUCTION

Myosin-V, an actin-based molecular motor, is involved in the trafficking of organelle and vesicles of the melanolysosomal pathway as well as compartments of the smooth endoplasmic reticulum and neurotransmitter vesicles [1, 2]. Class V myosin is composed of at least three members, myosin-Va, myosin-Vb, and myosin-Vc, in humans and other vertebrates [2]. Mutations in the myosin-Va human gene, located at the 15q21 chromosome, lead to a rare autosomal, recessive disorder called Griscelli syndrome (GS) [3]. The same disorder is observed when the *RAB27a* gene is mutated [4, 5]. Recent papers have demonstrated that there are important differences between the GS caused by *MYO5a* mutation (GS1) and that caused by *RAB27a* mutation (GS2). Both are characterized by an identical pigmentary dilution, resulting in silvery hair that is caused by aggregation of melanosomes in melanocytes. GS1 patients are marked by a severe, primary neurological impairment, whereas *Rab27a* mutations cause a haemophagocytic syndrome, characterized by periods of T-cell and macrophage activation that lead to lymphohistiocytic infiltration of many organs including the central nervous system, culminating in secondary neurological disorders and death in early childhood [5, 6]. Defective cytotoxic activity was found in *RAB27a* mutant T lymphocytes but not in *MYO5a* mutants [5]. Early bone marrow transplantation is the only successfully described treatment for this disease [7, 8]. Extensive studies have been described regarding myosin-V function in nervous and pigmentary systems, and its expression in leukocytes has been observed (unpublished results; [9, 10]). In the present work, we quantify the expression and determine the subcellular distribution of myosin-V in peripheral blood mononuclear cells (PBMC). We also show evidence from flow cytometry and Western blot analyses that the amount of myosin-V protein increases following T-lymphocyte activation. In addition, we show evidence from reverse transcription-polymerase chain reaction (RT-PCR) analysis that phytohemagglutinin (PHA) stimulation of T lymphocytes enhances expression of the three members of class V myosins (a, b, and c).

MATERIALS AND METHODS

Subjects

Whole blood samples were collected from a total of 37 consenting, healthy adult blood donors from the Blood Center of Ribeirão Preto (São Paulo, Brazil).

Antibodies

Monoclonal anti-human cluster of differentiation (CD) markers and antimajor histocompatibility complex (MHC) class II were purchased from Becton Dickinson (San Jose, CA). Monoclonal anti-β-tubulin, anti-DLC8, and anti-LAMP-1 were obtained from Transduction Laboratories (Lexington, KY). Monoclonal antibody (mAb) to γ-tubulin was purchased from Sigma Chemical

Correspondence: Enilza M. Espreafico, Av. Bandeirantes, 3900, Ribeirão Preto, SP, 14049-900, Brazil. E-mail: emesprea@fmrp.usp.br

Received April 1, 2001; revised October 4, 2001; accepted October 5, 2001.

Co. (St. Louis, MO). We used two affinity-purified rabbit polyclonal antibodies against chicken myosin-Va: the antibody raised to the recombinant tail protein (32a clone) [11] for the first flow cytometry analysis in cell subpopulations and for all the other analyses, an antibody raised against the medial-tail region, which has been shown to be highly specific to a polypeptide of 190 kDa in whole brain and melanoma cell extracts and to give a staining pattern equivalent to the anti-32a antibody in cells and tissues (unpublished results). Secondary antibodies conjugated with fluorescein isothiocyanate (FITC) or Texas Red were obtained from Molecular Probes (Junction City, OR).

Cell isolation

PBMC were freshly isolated from whole heparinized blood by Ficoll-Hypaque density-gradient technique (HYSTOPAQUE-1077; Sigma Chemical Co.). Fresh, isolated cells were immunolabeled for flow cytometry or confocal microscopy analyses, or they were taken into culture as described below.

Immunolabeling and flow cytometry

Mononuclear cells from 19 healthy donors were used in these assays. Cells were washed three times in phosphate-buffered saline (PBS), pH 7.2, and resuspended in PBS at a density of 5×10^9 cells/L. Cell-surface labeling was performed by a direct fluorescence technique, in aliquots of 100 μl cell suspension, using 5 μl each of the phycoerythrin (PE)-conjugated mAb (Becton Dickinson) against human CD3 (T lymphocyte), CD4 (T-helper lymphocytes), CD8 (T-cytotoxic lymphocytes), CD16 [natural killer (NK) cells], CD19 (B lymphocytes), CD56 (NK cells), and CD14 (monocytes), respectively. Labeled mononuclear cells were washed three times with PBS, followed by fixation and permeabilization in the same buffer containing 2% paraformaldehyde and 0.01% saponin during 10 min at 37°C. After washing three times, they were blocked for 1 h in PBS containing 2% bovine serum albumin (BSA) and 5% goat serum and labeled by an indirect fluorescence technique with antimyosin-Va and a FITC-conjugated anti-rabbit immunoglobulin G (IgG), both diluted at ~10 μg/ml in blocking solution. Both incubations were performed for 1 h followed by four times washing with PBS. As a control for nonspecific staining and to set the background level, cells were labeled under the same conditions as specified above with PE- and FITC-conjugated γ1γ2 antibody. Flow cytometry analyses were carried out on FACSORT equipment (Becton Dickinson) using a linear amplifier with a resolution of 1024 and the CELLQUEST analysis software. Fluorescence intensity was expressed in arbitrary units (number of channel-shifting) in a histogram plot on a 0–1023 linear scale for 10,000 cells counted in the lymphocyte gate and 15,000 in the monocyte gate per blood sample analyzed. The results were expressed as the median of fluorescence intensity, calculated from 10,000 or 15,000 cells, subtracted from the background fluorescence, for each cell subpopulation from each one of the 19 blood samples analyzed, i.e., median of number of channel-shifting from isotype control.

Immunolabeling and confocal microscopy

Cells were plated on Cell-Tak (Becton Dickinson)-treated glass coverslips inside 35-mm diameter Petri dishes. For the colabeling studies with the CD markers, immunostaining was done as described above for flow cytometry. For all the other colabeling assays, cells were fixed and permeabilized as described above and then incubated with blocking solution (2% BSA, 5% goat serum in PBS) for 1 h at room temperature, followed by incubation with the primary antibodies (~10 μg/ml) diluted in blocking solution, for 1 h at 37°C. Cells were washed four times with PBS, incubated for 30 min at 37°C with the secondary antibodies (10 μg/ml in blocking solution), FITC- or Texas Red-conjugated, and then washed again with PBS, pH 8.3. Coverslips were mounted in 1 mg/ml *p*-phenylenediamine in 90% glycerol and PBS and analyzed in a Leica confocal system, using Leica TCS-NT software (Leica, Microsystems Heidelberg GmbH, Germany) for image acquisition and processing.

Lymphocyte stimulation with PHA or OKT3 antibody

Freshly isolated PBMC from 18 healthy subjects were cultured in RPMI-1640 medium (Sigma Chemical Co.) supplemented with L-glutamine (2 mM), 10% decomplemented fetal bovine serum, penicillin (100 units/ml), and streptomycin (100 μG/ml) at a density of 2.5×10^9 cells/L in a flat-bottomed, 24-well plate (Costar, Cambridge, MA) in a humidified atmosphere with 5% CO_2 at 37°C. For lymphocyte stimulation, the culture medium was supplemented with 10 μl OKT3 mAb to CD3 (Ortho Biotech Products, LP) or with 2.5 μg/ml PHA (Sigma Chemical Co.). Cells were cultured for 24 h for OKT3 or during a period of 72 h for PHA stimulation. Nonstimulated cells cultured for 72 h were tested for viability in flow cytometry by the Annexin-V-FITC staining, using the APOPTEST-FITC protocol (A-700) and propidium iodide staining (Nexins Research B.V.). Viability above 95% was obtained.

Flow cytometry analysis in resting and activated T lymphocytes

To evaluate the effect of T-lymphocyte activation on myosin-Va expression, we analyzed fluorescence intensity for myosin-Va staining in CD3+ lymphocytes. Mononuclear cells were isolated from a total number of 18 blood samples and were cultured as specified. Immunolabeling procedures and fluorescein-activated cell sorter (FACS) analysis for CD3 and myosin-Va staining were done as described above. To confirm activation, cells were coimmunolabeled for CD3 and CD69 or CD3 and HLA-DR by a direct fluorescence technique with mAb, conjugated with FITC or PE. The antibody to HLA-DR was directed to a monomorphic region. FACS analysis was done as explained above, and the results were expressed as % of stained cells (above background levels) for CD69 and HLA-DR and median of fluorescence intensity for myosin-Va staining.

Immunoblotting

Cells were cultured as described above for 72 h, without or with the addition of PHA, in 25 cm^2-vented flasks. After this period, cells were washed in PBS and resuspended in 1 ml PBS, and an aliquot of the cell suspension was taken for cell counting in a Neübauer chamber in the presence of Trypan blue staining. (Near 100% viability was obtained in both cultures.) Cell suspension volume was raised to obtain 1×10^6 cells/ml, 1 ml each cell suspension was spun, and the pelleted cells were homogenized directly in 100 μl sodium dodecyl sulfate-polyacrylamide gel electrophoresis (SDS-PAGE) sample buffer (2× concentrated), boiled for 10 min, spun briefly, ultrasonicated 3×5 s, and spun for 10 min. A serial dilution of 2, 4, and 8 times was performed for both samples. A volume of 10 μl from each dilution, containing the amount of total protein, respectively, from 1, 0.5, 0.25, and 0.125×10^5 cells, was subjected to SDS-PAGE on 6–21% acrylamide gels. Electrophoresed proteins from one gel were transfered to 0.22 μm nitrocellulose using a Hoeffer transfer apparatus for 12 h at 200 mA. An identical gel was subjected to protein staining with SyproOrange (Molecular Probes) diluted at 1:5000 in 7.5% acetic acid for 40 min under slow agitation protected from room light. Gel was briefly washed (5 min) in 7.5% acetic acid and scanned in a Storm instrument from Molecular Dynamics (Sunnyvale, CA), and the total protein on each lane was analyzed based on the optical density (OD) using the ImageQuant software. The results were expressed as % of OD, relative to the sum of OD values (100%) for the eight lanes in the gel, including the nonstimulated and PHA-stimulated cells. The analysis indicated that equivalent amounts of total protein for stimulated and nonstimulated cells were loaded on the gels. The nitrocellulose membrane was subjected to immunodetection assay for myosin-Va and γ-tubulin simultaneously as follows. The membrane was blocked in 5% nonfat milk in Tris-buffered saline (TBS) with 0.2% Tween-20 (TBS-T) for 1 h at room temperature and then was incubated with affinity-purified polyclonal antibody to the medial tail of myosin-Va diluted at 1 μg/ml and a mAb to γ-tubulin (clone GTU-88) 1:2000 in TBS-T for 2 h at room temperature. After the wash, the membrane was incubated for 1 h with goat anti-rabbit or goat anti-mouse peroxidase-conjugated secondary antibodies (Promega, Madison, WI), diluted at 1:2500 in blocking buffer, and developed using the enhanced chemiluminescence (ECL) Western blotting detection reagent (Amersham Pharmacia Biotech, Little Chalfont, UK) and Kodak BIOMAX Light-1 film, according to the manufacturer's directions. For myosin-Va detection, the membrane exposed to the chemiluminescent substrate was allowed exposure to film for ~20 s, and for γ-tubulin detection, the exposure was 1–2 s. OD for each band in the gel was measured by using the ImageJ software, a Java port to NIH Image (http://rsb.info.nih.gov/nih-image/), on a PC using the Linux operational system. The results were expressed as % of OD relative to the sum (100%) of the eight OD values obtained for each protein (four dilutions from each of the cell samples).

RNA preparation and RT-PCR analysis

Cells were cultured for 72 h in 5 ml medium, without or with the addition of PHA, in 25 cm^2-vented culture flasks. For total RNA extraction, cell suspensions were spun, and the cell pellets were homogenized quickly in 1 ml Trizol (Life Technologies, Gibco-BRL, Paisley, UK), according to the manufacturer's directions, except that precipitation was done overnight at −20°C. Dry RNA pellets were dissolved in diethyl pyrocarbonate-treated water and quantified by spectrophotometer analysis at 260/280 nm. For RT-PCR, total RNA was treated with DNAse I (Promega) at 1 U/2 μg total RNA in 10 μl reaction volume and incubated for 30 min at 37°C, followed by enzyme inactivation by the addition of 1 μl 20 mM ethyleneglycol-bis(β-aminoethylether)-*N,N'*-tetraacetic acid (EGTA) and incubation for 15 min at 65°C. cDNA synthesis was performed for three different amounts of total RNA (2.0, 0.2, and 0.04 μg) in 20 μl reaction with the Superscript II Reverse Transcriptase (Life Technologies, Gibco-BRL), according to the manufacturer's instructions, using 4 μl 5× first-strand buffer, 1 μl 10 mM dNTP, 200 U Superscript II enzyme, 2 μl 0.1 M dithiothreitol (DTT), and 250 nG oligo dT primer (Life Technologies, Gibco-BRL). For PCR reactions, 1 μl each synthesized cDNA was used as template in a reaction volume of 25 μl containing 200 μM dNTPs, 1.5 mM $MgCl_2$, 0.25 μM each primer, and 1 U Taq DNA polymerase in the manufacturer's recommended buffer (Life Technologies, Gibco-BRL). The reaction was allowed to denature for 4 min at 94°C followed by amplification. For myosin-Va and β-actin amplification, 34 cycles (1 min at 94°C, 1 min at 55°C, and 1 min at 72°C) were done, whereas 40 cycles of amplification were done for myosin-Vb and myosin-Vc (1 min at 94°C, 1 min at 55°C, and 1 min at 72°C). In all cases, polymerase chain reaction (PCR) was terminated by incubation for a further 10 min at 72°C. Amplification of β-actin cDNA was done as control of mRNA content. Human brain cDNA and HeLa cells cDNA were used as positive controls and reference samples. The following forward (F) and reverse (R) primers were used for amplification: F-agtctctgtgtcgttcattcg and R-cctgtatgtaaactcacggta for myosin-Va; F-taactcatactgcctggaagc and R-acttccttcttgctcacattg for myosin-Vb; F-agacagtgatgccaaggaga and R-gagtgagagatgatgtggtc for myosin-Vc; and F-ggcatcgtgatggactccg and R-gctggaaggtggacagcga for β-actin. Equal volume (5 μl) of each PCR product was loaded on a 1% agarose gel and electrophoresed in TAE buffer (40 mM Tris-acetate, pH 8.0, 1 mM EDTA). Gels were subjected to ethidium bromide staining and were imaged in a UV transilluminator using a digital Kodak camera.

RESULTS

Myosin-V is expressed in the major subtypes of mononuclear cells

Fluorescence intensity for myosin-Va staining was determined for seven subsets of mononuclear cells isolated from 19 blood donors (**Fig. 1**). All of the cell subtypes analyzed ($CD3^+$, $CD4^+$, $CD8^+$, $CD19^+$, $CD16^+$, $CD56^+$, and $CD14^+$) were positively labeled for myosin-V: The percentages of stained cells for each cell subset corresponded approximately to the cellular composition of the PBMC in each of the 19 blood samples analyzed, as determined by the CD markers coimmunostaining (unpublished results). The nonparametric test analysis of Friedman and Wilcoxon performed on the 19 blood samples (Fig. 1) showed no statistically significant difference in fluorescence intensity for myosin-V between $CD3^+$ lymphocytes and $CD14^+$ monocytes ($P=0.8038$); NK ($CD16^+$ and $CD56^+$) and $CD14^+$ monocytes ($P=0.0857$); $CD19^+$ lymphocytes and $CD14^+$ monocytes ($P=0.5263$); and $CD4^+/CD8^+$ lymphocytes and $CD19^+$ lymphocytes ($P=0.5034$). A statistically significant difference ($P=0.0251$) in fluorescence intensity between $CD56^+$ NK cells and all the lymphocyte subsets and monocytes was observed.

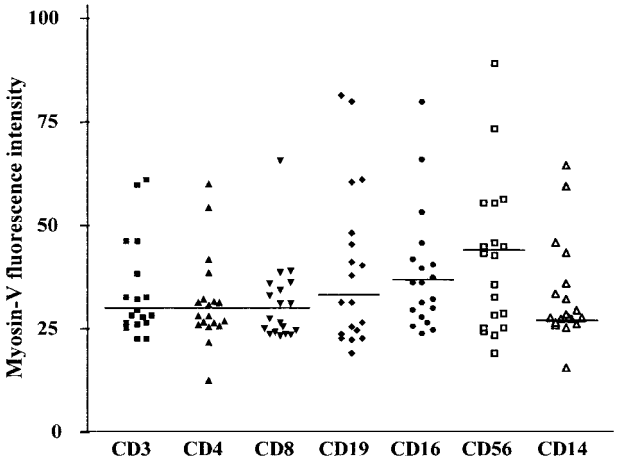

Fig. 1. Flow cytometric analysis of fluorescence intensity for myosin-V labeling in PBMC. Each of the data points plotted in this figure represents the median value of fluorescence intensity from 10,000 lymphocytes or NK cells or 15,000 monocytes counted minus background fluorescence of isotype control from each of the 19 healthy blood donors. Fluorescence intensity was measured in arbitrary units (channel-shifting) on a linear scale of 0–1023. Horizontal lines represent the median value from the 19 data points. The different symbols representing the data points correspond to the different cell subsets indicated on the *x*-axis. The median of the background fluorescence intensity for each cell subpopulation was 14.64 for lymphocytes (CD3, CD4, CD8, CD19) and NK cells (CD16, CD56) and 22.67 for monocytes. There is no statistically significant difference between CD3+ lymphocytes and monocytes ($P=0.8038$), NK and monocytes ($P=0.0857$), and CD19+ lymphocytes and monocytes ($P=0.5263$). The median intensity for NK cells is higher when compared with the median for all the lymphocyte subsets and monocytes together ($P=0.0251$).

Subcellular distribution of myosin-V

Confocal microscopy was performed to confirm the presence and determine the cytoplasmic distribution of myosin-V in PBMC, by reconstruction from multiple optical sections (**Fig. 2**, columns A–C) or in single sections (**Fig. 3D**). All of the cells, differentiated by the CD markers (red), were labeled for myosin-V (green) in a very similar punctate pattern of staining. This staining was shown to be concentrated at one spot in the cell and also distributed throughout the cytoplasm (Fig. 2). Double-labeling of myosin-V and β-tubulin confirmed that the more conspicuous spot-like staining for myosin-V coincided with the microtubule-organizing center (Fig. 3A). In addition, myosin-V puncta were found on straight paths aligned with the central microtubule arrays (Fig. 3A). Figure 3B shows that myosin-V puncta also colocalize with actin-filament staining, which is enriched at the peripheral-ruffled region in these cells. In an attempt to determine the nature of these myosin-V puncta, we performed colocalization studies with several markers. Colocalization with the endolysosomal marker lamp-1 (Fig. 3C) as well as with the 8 k dynein light chain, DLC8 (Fig. 3D), was found mostly restricted to the centrosomal region in both cases. It is interesting that in most cells, we observed that the myosin-V-stained puncta are present even at the outermost cortical region, probably just subjacent to the plasma membrane. These puncta were found especially to colocalize quite extensively with the punctate staining for MHC class II molecules (**Fig. 4**). These molecules are carried to the cell surface on vesicles from the trans Golgi network and most importantly

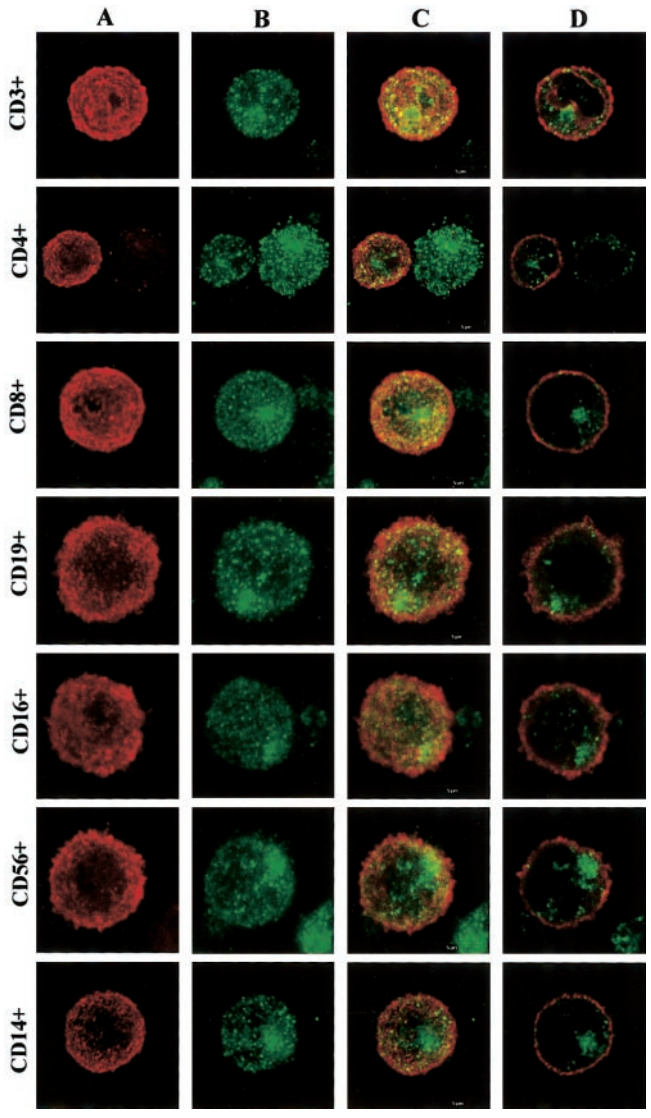

Fig. 2. Cellular distribution of myosin-V imaged by confocal microscopy in PBMC. (A–C) 3-D Maximal projection images from multiple optical sections. (A) CD markers; (B) myosin-V labeling; (C) superimposed labeling of A and B images; (D) single optical section overlaid images of myosin-V and CD-marker labeling. Note that myosin-V staining shows a granular pattern throughout the cytoplasm with an accumulation in a restricted perinuclear region. All cell subtypes are stained for myosin-V in agreement with the flow cytometry analysis.

on vesicles derived from the endocytic compartments following the pathways of antigen-loading and recycling (for review, see ref. [12]). We also noted intense staining for myosin-V in cellular fragments suggestive of platelets (Figs. 2–4).

The amount of myosin-V increases following T-lymphocyte activation

Having determined that myosin-V colocalizes with the endocytic marker, lamp-1, and especially with MHC class II in mononuclear cells, we asked whether the amount of myosin-V protein would be affected upon T-lymphocyte activation by PHA or OKT3 antibody, which induces MHC class II expression. To demonstrate that PHA or OKT3 activation occurred, we determined the expression of HLA-DR and CD69 in resting and activated $CD3^+$ lymphocytes by flow cytometry (**Fig. 5**). The percentage of HLA-DR- and CD69-stained cells increased significantly after PHA or OKT3 activation (Fig. 5, A and B). Under the same conditions, we analyzed the fluorescence intensity for myosin-V staining in cells from 17 blood samples for PHA activation and 7 blood samples for OKT3 activation. As explained in Figure 1, fluorescence intensity was measured for 10,000 cells in each data flow file, and the results were expressed as the median of the fluorescence intensity subtracted from the background for each blood sample (Fig. 5C). As shown in Figure 5C, PHA- or OKT3-activated T lymphocytes exhibited a significant increase in myosin-V fluorescence intensity when compared with resting cells. To verify whether the increase in myosin-V fluorescence intensity in PHA-activated lymphocytes in fact reflects an increase in the amount of myosin-V, we performed immunoblot analysis for resting and PHA-activated cells. Cell homogenates were prepared from an equal number of cells from both cultures. SyproOrange staining revealed that equivalent amounts of total protein were loaded on gels for resting or PHA-activated cells (**Fig. 6, A** and **D**), whereas immunoblot analysis (Fig. 6, B and D) revealed a more intense signal for myosin-V staining (~2.5 times greater, by averaging the four dilutions) in samples from PHA-stimulated cells when compared with the nonstimulated (NS) cells. As an internal control of the relative amount of protein detected by immunoblotting in resting or activated cells, we performed simultaneous staining for γ-tubulin with a commercially available mAb. The γ-tubulin staining was ~1.5 times more intense in the stimulated cells. Therefore, we observed a still greater increase in the myosin-V staining compared with the γ-tubulin staining upon PHA stimulation. Several cytoskeleton-associated proteins have been demonstrated to increase upon T-lymphocyte activation [13].

T-lymphocyte activation up-regulates class V myosin expression

We used RT-PCR to assess the abundance of mRNA for myosin-Va, myosin-Vb, and myosin-Vc in nonstimulated and PHA-stimulated cells. **Figure 7** shows PCR products obtained from cDNA synthesized from three different amounts of total RNA from donor 1 PBMC (2.0, 0.2, and 0.04 μg) for myosin-Va and β-actin amplification and two different amounts (2.0 and 0.2 μg) for myosin-Vb and myosin-Vc. Myosin-Va was also analyzed in PBMC from donor 2 using 2.0 and 0.2 μg total RNA. A single PCR product of the expected size was obtained for each reaction: 435 bp for myosin-Va, 650 bp for myosin-Vb, 440 bp for myosin-Vc, and 594 bp for β-actin. The pairs of primers for the three myosin-V members were designed to have the same melting temperature and to anneal to the same general region of the mRNA, flanking the stop codon. No PCR products were obtained in the absence of template, confirming the specificity and purity of the primers used (Fig. 7A, lane *T*−). We also verified that no PCR products were obtained in reactions of β-actin amplification using total RNA, DNase-treated, and not reverse-transcribed as template, confirming that the PCR products obtained are derived from cDNA and not from genomic DNA (unpublished results). PCR product was obtained from RNA samples from brain tissue and HeLa cells for myosin-Va and -Vb and only from HeLa cells for myosin-

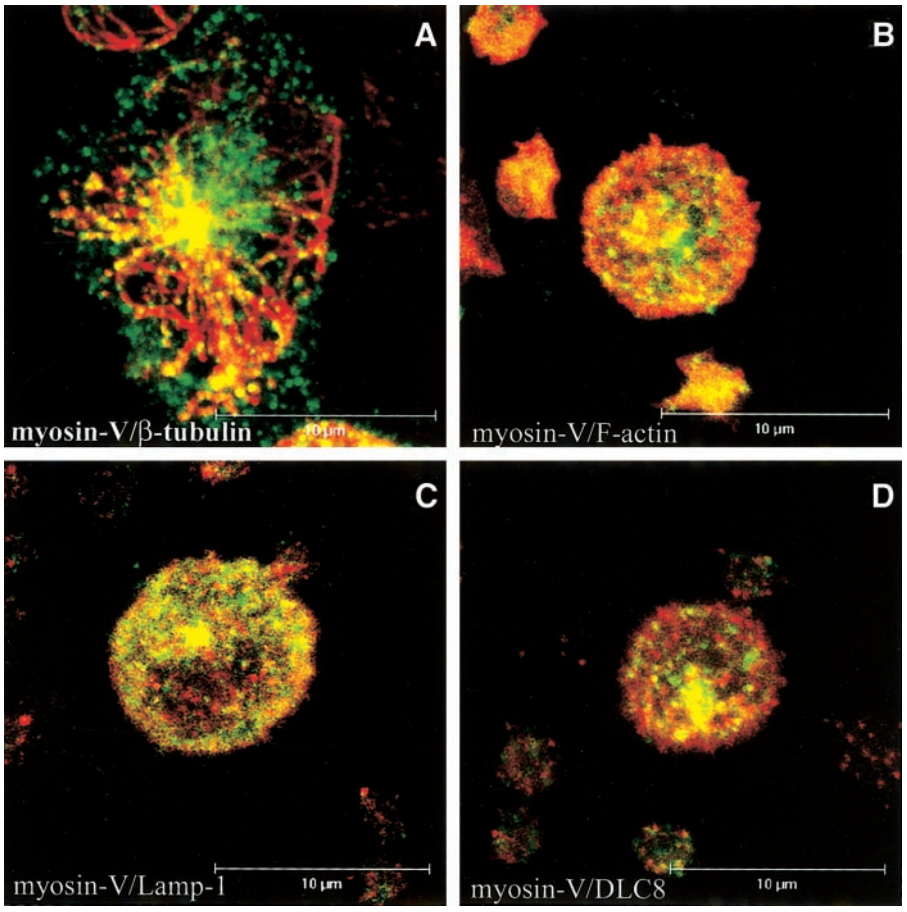

Fig. 3. Confocal microscopy analysis of the myosin-V colocalization with microtubules (A); F-actin (B); endolisosomal marker lamp-1 (C); and the 8-kDa dynein light chain (DLC8; D). Myosin-V staining is shown in green, and the staining for the other molecules is in red. Myosin-V was detected with the medial-tail antibody, microtubules with a mAb to β-tubulin, and F-actin with rhodamine-conjugated phalloidin. Note that a prominent myosin-V staining coincides with the centrosomal region and the central microtubules array. Puncta of myosin-V staining also colocalize with cortical actin-filament staining. Myosin-V staining present in the cell center showed colocalization with lamp-1 and DLC8.

Vc. We obtained abundant PCR product for myosin-Va (Fig. 7A) in nonstimulated and PHA-stimulated cells with 34 cycles of PCR compared with undetectable products for myosin-Vb and -Vc with the same number of cycles (unpublished results). Figure 7A also shows that the amount of myosin-Va PCR product is greater in the PHA-stimulated cells when compared with nonstimulated cells in samples from donors 1 and 2. Densitometric analysis of these gels (Fig. 7, B and C) using β-actin product for normalization shows an increase in the amount of myosin-Va PCR product of ~1.5 times in the case of donor 1 and 3–5 times in donor 2 in the PHA-stimulated cells as compared with nonstimulated cells. These results were confirmed in additional and independent RT-PCR assays from the same RNA samples (unpublished results). Detection of PCR products for myosin-Vb and -Vc was possible when amplification was done for 40 cycles (Fig. 7, D and F). It is interesting that in these conditions, we detected a low amount of PCR product for myosin-Vb (Fig. 7D) and no product for myosin-Vc (Fig. 7F) in the nonstimulated cells, whereas in PHA-stimulated cells, a great increase in the amount of myosin-Vb PCR product was obtained (~8 times, based on the densitometric analysis shown in Fig. 7E). The same result was obtained in additional RT-PCR experiments using the same RNA samples from donor 1 as well as from donor 2 (unpublished results). Myosin-Vc PCR product was only detected in the 2 μg RNA sample of the PHA-activated cells (Fig. 7C). Therefore, these results indicate that myosin-Va mRNA is by far the most abundant myosin-V mRNA in mononuclear cells and reveal an increase in the amount of mRNA for the three members of class V myosins following activation in T lymphocytes.

DISCUSSION

Myosin-V has been well-studied in yeast [14–16], melanocytes [17–19], and neurons [20–24], where it has been implicated in organelle and vesicle trafficking. However, myosin-V is also expressed in many other cell types, such as epithelial, glial, and neuroendocrine cells as well as leukocytes [9, 11, 25, 26]. Immune cells exhibit a diverse repertoire of dynamic cellular events that rely on the cytoskeleton, such as cell polarization, surface expression of recognition molecules, secretion, endocytosis, and phagocytosis. Previous studies showing that mutations in the *MYO5a* gene were present in patients with GS [3] made it important to characterize myosin-V in immune cells. In the present study, the levels of myosin-V expression among the major subtypes of blood mononuclear cells and the pattern of cytoplasmic distribution of myosin-V were determined. We used two affinity-purified antibodies (32a and medial tail) raised against chicken-brain myosin-V recombinant tail proteins to perform these studies. These antibodies are highly specific to myosin-V, recognizing a single band of ~190 k on Western blots containing crude extracts from melanocytes, whole brain, and leukocytes (unpublished results). Also, we have determined by immunohistochemistry (ongoing studies)

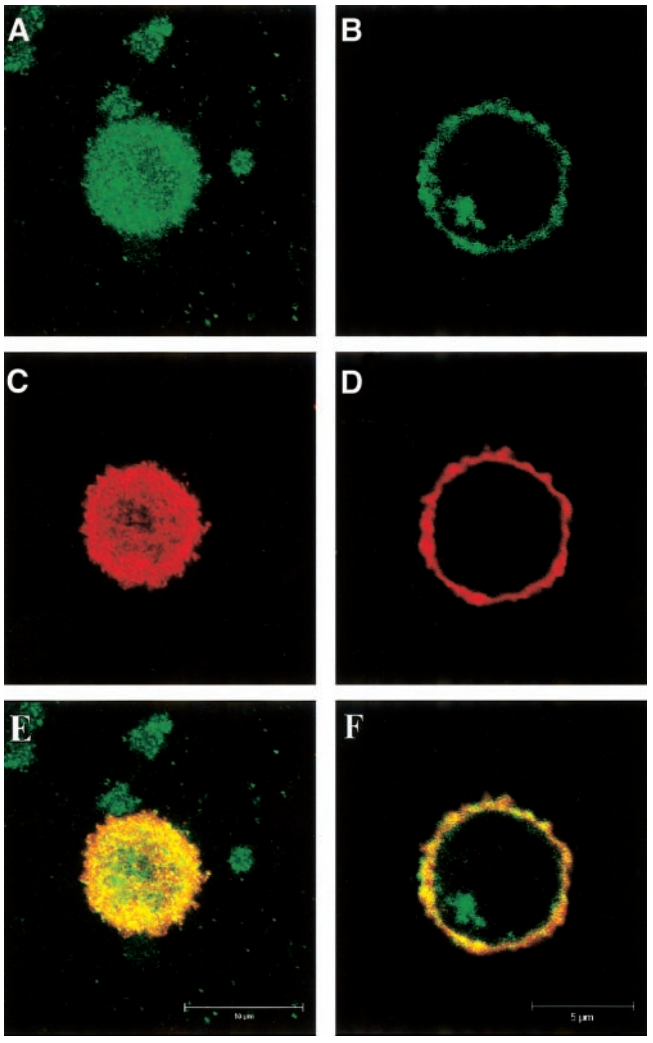

Fig. 4. Confocal microscopy analysis of the myosin-V colocalization with MHC class II molecules. (A, B) Myosin-V staining; (C, D) MHC class II staining; and (E, F) superimposed labeling. (A, C, E) Maximal projection from multiple optical sections. (B, D, F) Single optical sections. A striking centrosomal staining for myosin-V is particularly noted in a single optical section through the cell (B). MHC class II staining is concentrated on the cell surface (C, D) and is highly colocalized with myosin-V punctate staining (E, F), suggesting that myosin-V puncta are just subjacent to the plasma membrane.

that the medial-tail antibody exhibits a staining pattern similar to the one obtained for the previously characterized 32a antibody [11], which has been used extensively in studies from several laboratories. In addition, these antibodies exhibit a different pattern of cellular and tissue distribution than that shown for an antibody to myosin-Vb produced in our laboratory, which does not cross-react with myosin-Va. Therefore, this implies that the staining shown in leukocytes in the present work is not a result of recognition of myosin-Vb. In fact, probing of the Western blot shown in Figure 6 with the antibody to myosin-Vb gave a much fainter signal than the one detected with the antimedial tail (unpublished results). In addition, the mRNA expression analyses shown here (Fig. 7) also support the supposition that the myosin-V staining presented here is specific to myosin-Va, because myosin-Vb and -Vc appear to be expressed at much lower levels than myosin-Va in blood mononuclear cells.

In the present work, we demonstrate that the major cell subtypes of the PBMC, including cytotoxic and helper T lymphocytes, B lymphocytes, NK cells, and monocytes, do express myosin-V. The expression levels of myosin-V, as measured from the fluorescence intensity by flow cytometry, were shown

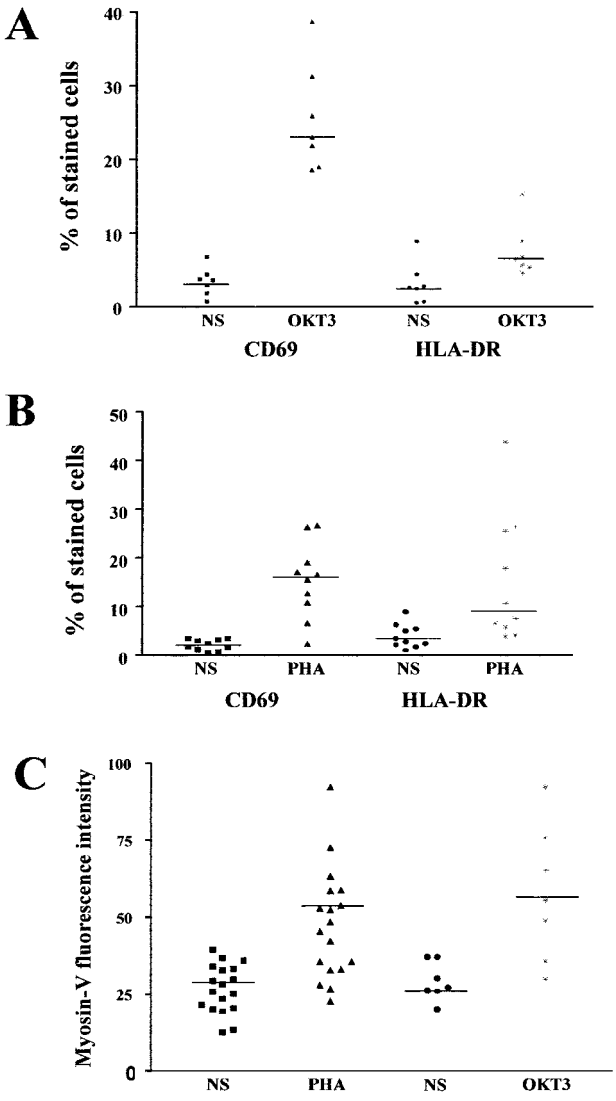

Fig. 5. Flow cytometric analysis of myosin-V fluorescence intensity in resting and activated T lymphocytes. (A) Percentage of HLA-DR- and CD69-positive T lymphocytes after 24 h in culture without stimulation (NS) or with stimulation with OKT3 mAb. (B) Percentage of HLA-DR- and CD69-positive T lymphocytes after 72 h in culture without stimulation (NS) or with stimulation with PHA. The increase observed in the number of T lymphcytes expressing CD69 and HLA-DR antigens following OKT3 or PHA stimulation was statistically significant ($P=0.015$ and $P=0.002$, respectively). (C) Fluorescence intensity for myosin-Va labeling of $CD3^+$ lymphocytes nonstimulated (NS) and stimulated with PHA or OKT3 antibody. Fluorescence intensity is expressed by the median intensity—background subtracted—calculated from 10,000 cells analyzed for each of the 17 blood samples for the PHA stimulation assay and 7 blood samples for the OKT3 stimulation assay. The symbols plotted represent the data points for different groups as indicated on the *x*-axis. Horizontal lines represent the median value from the data points plotted. Myosin-Va labeling was done using affinity-purified polyclonal antibody to the medial-tail domain of chicken myosin-Va (the same antibody used for confocal microscopy and Western blots). A significant increase is observed in myosin-Va fluorescence intensity in T lymphocyte following PHA ($P=0.0002$) or OKT3 antibody ($P=0.0156$) stimulation.

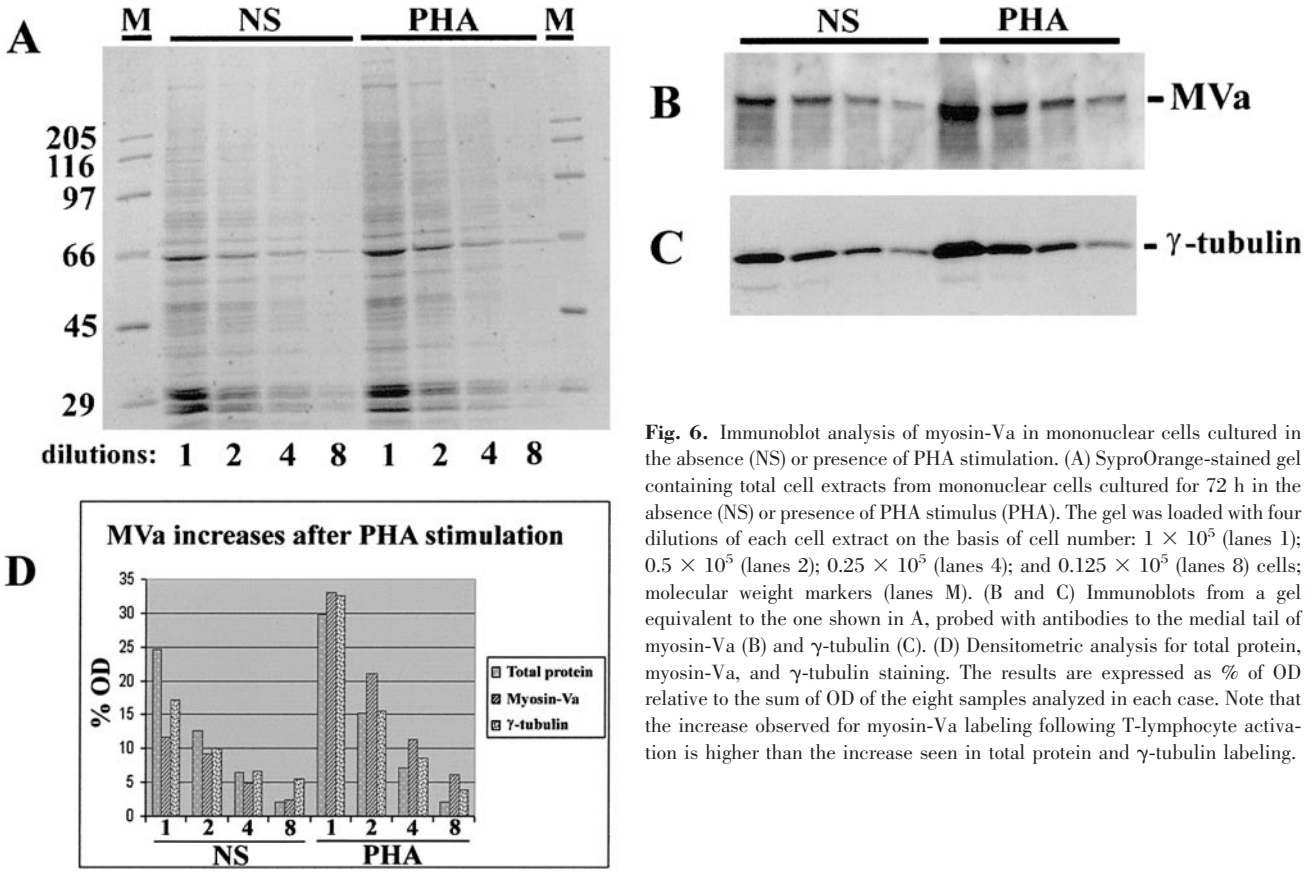

Fig. 6. Immunoblot analysis of myosin-Va in mononuclear cells cultured in the absence (NS) or presence of PHA stimulation. (A) SyproOrange-stained gel containing total cell extracts from mononuclear cells cultured for 72 h in the absence (NS) or presence of PHA stimulus (PHA). The gel was loaded with four dilutions of each cell extract on the basis of cell number: 1×10^5 (lanes 1); 0.5×10^5 (lanes 2); 0.25×10^5 (lanes 4); and 0.125×10^5 (lanes 8) cells; molecular weight markers (lanes M). (B and C) Immunoblots from a gel equivalent to the one shown in A, probed with antibodies to the medial tail of myosin-Va (B) and γ-tubulin (C). (D) Densitometric analysis for total protein, myosin-Va, and γ-tubulin staining. The results are expressed as % of OD relative to the sum of OD of the eight samples analyzed in each case. Note that the increase observed for myosin-Va labeling following T-lymphocyte activation is higher than the increase seen in total protein and γ-tubulin labeling.

to be basically equivalent among these cell types (Fig. 1). A slightly higher fluorescence intensity median was found for NK cells but also a greater dispersion of the data points than that seen for the other cell types. This may be suggestive of the existence of a subset of NK cells that express higher levels of myosin-V (Fig. 1).

A striking feature of the myosin-V staining in all mononuclear cells analyzed was the prominent staining at the centrosomal region (Figs. 2 and 3). Espreafico et al. [27], Wu et al. [28], and Tsakraklides et al. [29] have previously shown the presence of myosin-V in the centrosome of many cell lines. Immune responses require the participation of the centrosome, especially in the cell polarization event that takes place in NK cells and T lymphocytes. Ménasché et al. [5] have shown that mutations in the *RAB27a* gene but not in the *MYO5a* gene lead to deficient degranulation of cytotoxic T lymphocytes that might be responsible for the immunodeficiency in GS2 patients. Cell polarization is decisive for an efficient cytotoxicity of target cells. This is a particularly interesting aspect to investigate given the recent demonstration that the myosin-V in *Saccharomyces cerevisiae* (Myo2p) is required for spindle microtubule orientation [16]. An explanation for the lack of cytotoxicity defect in T lymphocytes of GS1 patients is that additional paralogs of myosin-V could be substituting for the lack of myosin-Va. Some redundancy of function has already been pointed out between myosin-Va and -Vb in neuronal cells [30].

The punctate pattern of fluorescence staining for myosin-V, observed in all mononuclear cells, is suggestive of association with large protein complexes or membranous vesicles and organelles. The colocalization of myosin-V with the dynein light-chain DLC8 at the centrosomal region does not indicate by itself a direct association of these proteins, because the microtubule-based motor complex, dynein, is also enriched at the centrosome. It is an intriguing question as to why this light chain is shared by the two motor systems [31–33]. The centrosomal staining also markedly colocalizes with the endolysosomal marker lamp-1 (Fig. 3) in a region where endolysosomal vesicles of the late recycling compartments are known to be located. MHC class II are antigen-presenting, surface molecules that are transported preferentially and recycled via endolysosomal vesicles. We show here a striking colocalization of these molecules with myosin-V in the cell periphery (Fig. 4). These data suggest that myosin-V could be involved in the pathway of MHC class II expression or recycling. To start addressing this hypothesis, we asked whether activation of T lymphocytes, which induces MHC class II expression, would be associated with changes in the expression of myosin-V. It is interesting that we found that a significant increase in the amount of myosin-V protein occurs following PHA or OKT3 activation of T lymphocytes (Figs. 5 and 6). The variation in the myosin-V fluorescence intensity, which was higher in the stimulated lymphocytes than in resting cells among the 17 blood samples analyzed, might reflect differences in the activation response of T cells from different healthy individuals (Fig. 5). Pastural et al. [4] has recently shown evidence from immunoprecipitation assays that the amount of myosin-V protein is augmented in human cells with mutation in the *RAB27a* gene.

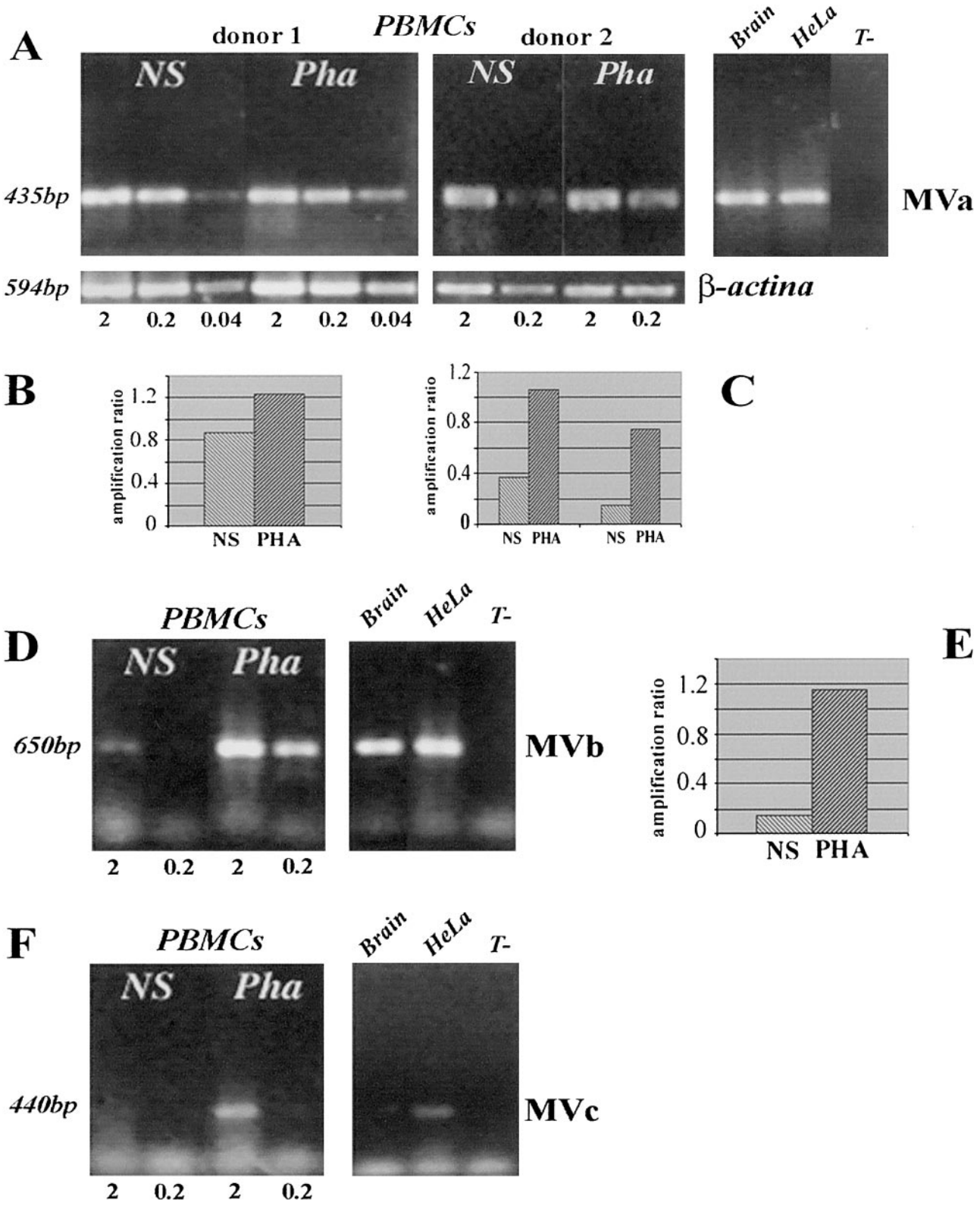

Fig. 7. RT-PCR from myosin-Va, myosin-Vb, and myosin-Vc mRNA in mononuclear cells cultured in the absence (NS) or presence of PHA stimulation. (A, D, F) Ethidium bromide-stained gels showing the RT-PCR products for myosin-Va and β-actin (A), myosin-Vb (D), and myosin-Vc (F), amplified from total RNA extracted from nonstimulated (NS) and PHA-stimulated mononuclear cells (PBMCs) from donors 1 and 2 for myosin-Va, from donor 1 for myosin-Vb and –Vc, and from human brain tissue and HeLa cells as indicated. The numbers below the lanes indicate the amount (μg) of total RNA used in the reverse-transcription reactions. PCR was done for 34 cycles for myosin-Va and β-actin and 40 cycles for myosin-Vb and myosin-Vc. "T-"indicates PCR in the absence of template. (B, C, E) Amplification ratio, calculated from the OD of the ethidium bromide-stained PCR products for myosin-Va from donor 1 (B), donor 2 (C), and myosin-Vb (E), normalized to the amount of β-actin PCR product detected in gel. Amplification ratio for myosin-Va, donor 1, was determined only based on the products in lanes 0.04 (NS, PHA), which did not show saturation of the PCR amplification, and for myosin-Vb, was determined based on the products in lanes 2 (NS and PHA), because no product was detected in lane 0.2, NS. The ratios shown here were confirmed in additional, independent experiments, using the same RNA preparations.

In light of the present results, it will be interesting to investigate in future studies a possible association of myosin-V with the uncontrolled cellular activation and proliferation that characterizes the immune defects in GS patients.

The possibility of functional redundancy among the class V myosin members and the demonstration that activation of T lymphocytes leads to an increase in the amount of myosin-V protein prompted us to extend our expression analysis to the level of mRNA and to include the three members of the class V myosins (a, b, and c). Our results indicate that mRNA for the three members of class V myosins is expressed in the PBMC and that myosin-Va mRNA is the most abundantly expressed, followed by myosin-Vb and -Vc, respectively (Fig. 7). In addition, this analysis suggests that there is an increase in the amount of myosin-Va mRNA following PHA stimulation, which was shown to vary from 1.5 times in one donor to 3–5 times in another donor. This variation is compatible with the variation in myosin-V fluorescence intensity detected in stimulated lymphocytes among different individuals (Fig. 5). It is interesting that despite the low levels of myosin-Vb and -Vc mRNA in PBMC, a pronounced increase was observed following mitogen activation, especially for myosin-Vb mRNA. Also at the level of protein expression, we observed an increase of the amount of myosin-Vb by probing the Western blot shown in Figure 6 with the antibody to myosin-Vb (unpublished results). It has recently been shown that myosin-Vb plays an important role in the expression of the IgA receptor to the plasma membrane in polarized and nonpolarized epithelial cells [34]. It is possible that myosin-Vb might also be required in similar processes, which are intense during cellular activation, in the immune response.

The myosin-V localization analysis shown here also indicated that many of the cytoplasmic particles stained for myosin-V in many of the cells analyzed on a given coverslip (Figs. 3 and 4 and unpublished results) do not colocalize with any of the markers used. It will be interesting to determine whether this important pool of myosin-V corresponds to lytic granules in cytotoxic T lymphocytes. The myosin-V staining that we show here is strikingly similar to the staining described by Haddad et al. [35] for granzyme B and Rab27a. Recently, it has been demonstrated that Rab27a is required to recruit myosin-Va to the melanosome surface, thereby allowing melanosomes to be anchored at the cell periphery [36–38]. Conversely, lymphocytes from dilute mice [35], as shown for GS1 lymphocytes, do not exhibit any defect in degranulation and cell cytotoxicity. It is remarkable that the *RAB27a* mutation leads to accumulation of lytic granules in cytotoxic T lymphocytes that fail to pass through the actin cytoskeleton and dock at the plasma membrane of the immunological synapse [39]. Together, these findings have led Stinchcombe et al. [39] to propose the hypothesis that class V myosins might be acting redundantly in lymphocytes, or residual amounts of functional myosin-Va would be present in the dilute or GS1 cells that have been analyzed. The pattern of localization of myosin-V shown here strengthens the idea that this myosin may play key roles in the motility/docking of vesicles at the plasma membrane and perhaps in the polarization toward the immunological synapse. In addition, the evidence that the expression of the three members of class V myosin is associated with the functional status of T lymphocytes supports the hypothesis that these myosins play relevant roles in the immune response, which might overlap to some extent, thus explaining the lack of immune defects associated with mutations in the *MYO5a* gene.

ACKNOWLEDGMENTS

This work was also supported by grants to R. E. L. and E. M. E. from the Fundação de Amparo à Pesquisa do Estado de São Paulo (FAPESP, 99/03951-7), Conselho Nacional de Desenvolvimento Científico e Tecnológico (CNPq), Fundação de Apoio ao Ensino, and Pesquisa e Assistência do Hospital das Clínicas da F.M.R.P.U.S.P. (FAEPA), FUNDHERP, and a grant to J. C. S. B. from the University of Ribeirão Preto—UNAERP. J. F. S. is the recipient of a doctorate fellowship from CAPES, and A. D. D. receives a fellowship from FAPESP. We especially thank Silmara Reis Banzi and Benedita Oliveira de Souza for technical assistance. We thank Marco Aurélio Valtas Cunha for precious help on computer management and Márcia Sirlene Zardin Graeff for assistance on the confocal microscope in the Department of Cellular and Molecular Biology and Pathogenic Bioagents of the Faculty of Medicine of Ribeirão Preto (FAPESP, 95/06199-3). We also thank the neurosurgeon Dr. Carlos Gilberto Carlotti Júnior as well as Dr. Luciano Neder Serafini, Dr. Maria Luisa Paço-Larson, and Valéria Valente for providing us with RNA sample from human brain tissue.

REFERENCES

1. Titus, M. A. (1997) Unconventional myosins: new frontiers in actin-based motors. Trends Cell Biol. 7, 119–123.
2. Reck-Peterson, S. L., Provance Jr., D. W., Mooseker, M. S., Mercer, J. A. (2000) Class V myosins. Biochim. Biophys. Acta 1496, 36–51.
3. Pastural, E., Barrat, F. J., Dufoureq-Lagelouse, R., Certain, S., Sana, O., Jabado, N., Seger, R., Griscelli, C., Fisher, A., Saint Basile, G. (1997) Griscelli disease maps to chromosome 15q21 and is associated with mutations in myosin-Va gene. Nat. Genet. 16, 289–292.
4. Pastural, E., Ersoy, F., Yalman, N., Wulffraat, N., Grillo, E., Ozkinay, F., Tezcan, I., Gedikoglu, G., Philippe, N., Fisher, A., de Saint Basile, G. (2000) Two genes are responsible for Griscelli syndrome at the same 15q21 locus. Genomics 63, 299–306.
5. Ménasché, G., Pastural, E., Feldmanm, J., Certain, S., Ersoy, F., Dupuis, S., Wulffraat, N., Bianci, D., Fisher, A., de Saint Basile, G. (2000) Mutations in RAB27a cause Griscelli syndrome associated with hemophagocytic syndrome. Nat. Genet. 25, 173–176.
6. Sain Basile, G. (2000) Implication du trafic intracellulaire dans trois maladies héréditaires du système hématopoïétique. Médicine/Sciences 16, 745–750.
7. Shneider, L. C., Berman, R. S., Shea, C. R., Perez-Atayde, A. R., Weinstein, H., Geha, R. S. (1990) Bone marrow transplantation (BMT) for the syndrome of pigmentary dilution and lymphohistiocytosis (Griscelli's Syndrome). J. Clin. Immunol. 10, 146–153.
8. Tezcan, I., Sanal, Ö., Ersoy, F., Uckan, D., Kilic, S., Metin, A., Cetin, M., Akin, R., Öner, C., Tuncer, A. M. (1999) Successful bone marrow transplantation in case of Griscelli disease which presented in accelerated phase with neurological involvement. Bone Marrow Tranplant. 24, 931–933.
9. Lambert, J., Naeyaert, J. M., Callens, T., De Paepe, A., Messiaen, L. (1998) Human myosin V gene produces different transcripts in a cell type-specific manner. Biochem. Biophys. Res. Commun. 252, 329–333.
10. Reis, D., Souza, M., Mineo, J., Espindola, F. (2001) Myosin V and iNOS expression is enhanced in J774 murine macrophages treated with IFN-gamma. Braz. J. Med. Biol. Res. 34, 221–226.

11. Espreafico, E. M., Cheney, R. E., Matteoli, M., Nascimento, A. A. C., De Camilli, P. V., Larson, R. E., Mooseker, M. S. (1992) Primary structure and cellular localization of chicken brain myosin-V (p190), an unconventional myosin with calmodulin light chains. J. Cell Biol. 119, 1541–1558.
12. Geuze, J. H. (1998) The role of endosomes and lysosomes in MHC class II functioning. Immunol. Today 19, 282–287.
13. Herblot, S., Chastagner, P., Samady, L., Moreau, J-L., Demaison, C., Froussard, P., Liu, X., Bonnet, J., Thèze, J. (1999) IL-2-dependent expression of genes involved in cytoskeleton organization, oncogene regulation, and transcriptional control. J. Immunol. 162, 3280–3288.
14. Johnston, G. C., Prendergast, J. A., Singer, R. A. (1991) The *Saccharomyces cerevisiae MYO2* gene encodes an essential myosin for vectorial transport of vesicles. J. Cell Biol. 113, 539–551.
15. Govindan, B., Bower, R., Novick, P. (1995) The role of MYO2, a yeast class V myosin, in vesicular transport. J. Cell Biol. 128, 1055–1068.
16. Yin, H., Pruyne, D., Huffaker, T. C., Bretscher, A. (2000) Myosin V orientates the mitotic spindle in yeast. Nature 406, 1013–1015.
17. Provance Jr., D. W., Wei, M., Ipe, V., Mercer, J. A. (1996) Cultured melanocytes from dilute mutant mice exhibit dendritic morphology and altered melanosome distribution. Proc. Natl. Acad. Sci. USA 93, 14554–14558.
18. Nascimento, A. A. C., Amaral, R. G., Bizario, J. C., Larson, R. E., Espreafico, E. M. (1997) Subcellular localization of myosin-V in the B16 melanoma cells, a wild-type cell line for the dilute gene. Mol. Biol. Cell 8, 1971–1988.
19. Wu, X., Bowers, B., Rao, K., Wei, Q., Hammer III, J. A. (1998a) Visualization of melanosome dynamics within wild-type and dilute melanocytes suggests a paradigm for myosin V function in vivo. J. Cell Biol. 143, 1899–1918.
20. Dekker-Ohno, K., Hayasaka, S., Takagishi, Y., Oda, S., Wakasugi, N., Mikoshiba, K., Inouye, M., Yamamura, H. (1995) Brain Res. 714, 226–230.
21. Wang, F-S., Wolenski, J. S., Cheney, R. E., Mooseker, M. S., Jay, D. G. (1996) Function of myosin-V in filopodial extension of neuronal growth cones. Science 273, 660–663.
22. Evans, L. L., Hammer, J., Bridgman, P. C. (1997) Subcellular localization of myosin V in nerve growth cones and outgrowth from dilute-lethal neurons. J. Cell Sci. 110, 439–449.
23. Costa, M. C. R., Mani, F., Santoro Jr., W., Espreafico, E. M., Larson, R. E. (1999) Brain myosin-V, a calmodulin-carrying myosin, binds to calmodulin-dependent protein kinase II and activates its kinase activity. J. Biol. Chem. 274, 15811–15819.
24. Bridgman, P. C. (1999) Myosin-Va movements in normal and dilute-lethal axons provide support for a dual filament motor complex. J. Cell Biol. 146, 1045–1060.
25. Espindola, F. S., Espreafico, E. M., Coelho, M. V., Martins, A. R., Costa, F. R. C., Mooseker, M. S., Larson, R. E. (1992) Biochemical and immunological characterization of p190-calmodulin complex from vertebrate brain: a novel calmodulin-binding myosin. J. Cell Biol. 118, 359–368.
26. Wolff, P., Abreu, P. A. E., Espreafico, E. M., Costa, M. C. R., Larson, R. E., Ho, P. L. (1999) Characterization of myosin V from PC12 cells. Biochem. Biophys. Res. Commun. 262, 98–102.
27. Espreafico, E. M., Coling, D. E., Tsakraklides, V., Krogh, K., Wolenski, J. S., Kalinec, G., Kachar, B. (1998) Localization of myosin-V in the centrosome. Proc. Natl. Acad. Sci. USA 95, 8636–8641.
28. Wu, X. F., Kocher, B., Wei, Q., Hammer, J. A. (1998b) Myosin-Va associates with mirotubule-rich domains in both interphase and dividing cells. Cell Motil. Cytoskelet. 40, 286–303.
29. Tsakraklides, V., Krogh, K., Wang, L., Bizario, J. C. S., Larson, R. E., Espreafico, E. M., Wolenski, J. S. (1999) Subcellular localization of GFP-myosin-V in live mouse melanocytes. J. Cell Sci. 112, 2853–2865.
30. Bridgman, P. (2000) Multiple roles for myosin V in synaptic function? I. International Symposium on Myosin V. II. Iberoamerican Forum on the Cytoskeleton, Paraty, RJ, Brasil.
31. Espindola, F. S., Suter, D. M., Partata, L. B., Cao, T., Wolenski, J. S., Cheney, R. E., King, S. M., Mooseker, M. S. (2000) The light chain composition of chicken brain myosin-Va: calmodulin, myosin-II essential light chains, and 8 kDa dynein light chain/PIN. Cell Motil. Cytoskelet. 47, 269–281.
32. Benashski, S. E., Harisson, A., Patel-King, R. S. (1997) Dimerization of the highly conserved light chain shared by dynein and myosin-V. J. Biol. Chem. 272, 20929–20935.
33. Jaffrey, S. R., Snyder, S. H. (1996) PIN: an associated protein inhibitor of neuronal nitric oxide synthase. Science 274, 774–776.
34. Lapierre, L. A., Kumar, R., Hales, C. M., Navarre, J., Bhartur, S. G., Burnette, J. O., Provance Jr., D. W., Mercer, J. A., Bahler, M., Goldering, J. R. (2001) Myosin Vb is associated with plasma membrane recycling systems. Mol. Biol. Cell 12, 1843–1857.
35. Haddad, E. K., Wu, X., Hammer III, J. A., Henkart, P. A. (2001) Defective granule exocytosis in Rab27a-deficient lymphocytes from Ashen mice. J. Cell Biol. 152, 835–841.
36. Hume, A. N., Collinson, L. M., Rapak, A., Gomes, A. Q., Hopkins, C. R., Seabra, M. C. (2001) Rab27a regulates the peripheral distribution of melanosomes in melanocytes. J. Cell Biol. 152, 795–808.
37. Bahadoran, P., Aberdam, E., Mantoux, F., Buscà, R., Bille, K., Yalman, N., Saint- Basile, G., Casaroli-Marano, R., Ortonne, J. P., Ballotti, R. (2001) Rab27a: a key to melanosome transport in human melanocytes. J. Cell Biol. 152, 843–849.
38. Wu, X. F., Rao, K., Bowers, M. B., Copeland, N. G., Jenkins, N. A., Hammer, J. A. (2001) Rab27a enables myosin Va-dependent melanosome capture by recruiting the myosin to the organelle. J. Cell Sci. 114, 1091–1100.
39. Stinchcombe, J. C., Barral, D. C., Mules, E. H., Booth, S., Hume, A. N., Machesky, L. M., Seabra, M. C., Griffiths, G. M. (2001) Rab27a is required for regulated secretion in cytotoxic T lymphocytes. J. Cell Biol. 152, 825–833.